JOURNAL OF GEOPHYSICAL RESEARCH, VOL. 88, NO. A12, PAGES 10,137–10,144, DECEMBER 1, 1983

Incoherent Scatter Measurements of Ion-Neutral Collision Frequencies and Temperatures in the Lower Thermosphere of the Auroral Region

CHANTAL LATHUILLERE

Centre d'Etudes des Phénomènes Aléatoires et Géophysiques

VINCENT B. WICKWAR

SRI International

WLODEK KOFMAN

Centre d'Etudes des Phénomènes Aléatoires et Géophysiques

Incoherent scatter observations performed in March and November 1978 at Chatanika have been used for studying the lower thermosphere in the auroral region. Neutral temperatures and densities have been found during periods without Joule heating. We present mean profiles of temperatures and collision frequencies (approximately proportional to neutral densities) for each month and profiles obtained during four specific nights. Between 93 km and 110 km the mean profiles of temperature are in good agreement with the Jacchia (1971) model, and the profiles of collision frequency are similar to those deduced from the model. Consistency checks between these collision frequencies and temperatures were performed, as were various simulations of the data. Neutral temperature profiles between 90 km and 140 km on the four specific nights show variations from one night to another that are not correlated to magnetic activity. However, there are systematic variations during each night that we suggest are due to atmospheric tides.

1. Introduction

The lower thermosphere is usually used as a limit zone for the thermospheric models: empirical models such as "Jacchia 71, 77" [*Jacchia*, 1971, 1977] or "MSIS" [*Hedin et al.*, 1977*a*, *b*] and theoretical models of auroral disturbance effects [e.g., *Mayr and Volland*, 1973]. Boundary conditions are often constant and given at an altitude of either 90 km or 120 km; however, neutral temperatures, densities, and compositions are quite variable in this region [*Offermann et al.*, 1981]. The aim of this paper is to show that the incoherent scatter technique is able to contribute to the understanding of the lower thermosphere in the auroral region by presenting first long-term results from Chatanika.

Already at middle and low latitudes, incoherent scatter radars have been extensively used for the study of the lower thermosphere: long-term variation studies [*Waldteufel*, 1970*a*; *Alcayde et al.*, 1979; *Salah et al.*, 1974; *Tepley and Mathews*, 1978] and short-term variation studies such as tides [*Bernard*, 1974; *Salah et al.*, 1975; *Wand*, 1976] and gravity waves [*Vidal-Madjar*, 1978]. At high latitudes, initial results were obtained by *Schlegel et al.* [1980].

In the second part of the paper, we recall how neutral temperatures and densities can be deduced from incoherent scatter measurements and examine the problems peculiar to the auroral zone. In the third part we present the results obtained with the Chatanika incoherent scatter radar. We describe the averaged temperature and density profiles obtained during two months of measurements: March 1978 and November 1978. We then examine the consistency of these profiles, first by assuming hydrostatic equilibrium and second by simulating the data. This latter check is performed because the altitude integration performed by the Chatanika multipulse correlator is larger than the neutral scale height. In the fourth part of this work, we present variations of collision frequency and temperature profiles observed during four specific nights. Finally, in the conclusion, we review the main results.

Paper number 3A1346.
0148-0227/83/003A-1346$05.00

2. Determination of Neutral Atmosphere Parameters With the Incoherent Scatter Technique

2.1. *Ion-Neutral Collision Frequency*

In the *E* region the incoherent scatter ion spectrum depends not only on the usual parameters (electron density N_e, electron and ion temperatures T_e and T_i, and ion velocity V_i) but also on the ion-neutral collision frequency ν_{in} [*Dougherty and Farley*, 1963; *Waldteufel*, 1970*b*]. This collision effect becomes negligible above an altitude of 110 km for the radar frequency used at Chatanika.

Theoretically, it is possible to deduce simultaneously the four parameters N_e, T_e, T_i, and ν_{in} from the incoherent scatter spectrum or the autocorrelation function, but the presence of much noise in the measurements makes a four-parameter regression practically impossible [*Lejeune*, 1980]. In particular, it is difficult to simultaneously determine the electron-to-ion temperature ratio and the ion-neutral collision frequency. However, *Schlegel et al.* [1980] show two such fits under conditions of large electron densities. We shall attempt to determine ν_{in} during periods when there is thermal equilibrium between electrons and ions: $T_e = T_i$. At middle and low latitudes, thermal equilibrium exists in the lower *E* region and its existence has been verified. However, at high latitude, different heating processes can disturb the thermal equilibrium. In the presence of particle precipitation, the electron temperature may be higher than the ion temperature; in the presence of electric fields the classical process of Joule heating will preferentially enhance the ion temperature, and a new heating mechanism due to unstable plasma waves (modified two-stream instability) will preferentially enhance the electron temperature [*St. Maurice et al.*, 1981].

Only this latter process is able to significantly change the thermal equilibrium below the altitude of 110 km. Indeed recent results from Chatanika show electron temperatures of 1200 K between 105 km and 110 km when ion temperatures remain between 250 K and 300 K [*Wickwar et al.*, 1981; *Schlegel and St. Maurice*, 1981]. During these periods of "elevated electron temperature," which are simultaneous to periods of high electric field, it will be impossible to determine the collision frequency ν_{in}.

2.2. *Neutral Temperature and Density*

The neutral temperature is deduced directly from the ion temperature determination, indeed the high value of the ion-neutral collision frequency below the altitude of 110 km ensures thermal equilibrium between ions and neutrals most of the time. However, during periods of very high electric field, Joule heating could raise the ion temperature above the neutral one: an electric field of approximately 40 mV/m would create a 20-K increase of T_i at 110-km altitude [*Banks and Kockarts*, 1973].

One must also keep in mind a possible enhancement of the ion temperature due to the modified two-stream instability heating process. This enhancement could be of the order of 30 K to 60 K in the *E* region [*St. Maurice et al.*, 1981]. Therefore great care must also be taken when studying neutral temperatures during periods of high electric field.

Neutral density and collision frequency are connected by

$$\bar{\nu}_{in} = 2.59 \times 10^{-9} n_n \left\{ \frac{\alpha_0}{\mu(i, n)} \right\}^{1/2} \quad (1)$$

[*Banks and Kockarts*, 1973], where $\bar{\nu}_{in}$ is the collision frequency for momentum transfer between ion species *i* and neutral species *n*, measured in the center of mass frame; n_n is the number density of neutral species *n*, $\mu(i, n)$ is the ion-neutral reduced mass (in atomic mass units), and α_0 is the neutral gas atomic polarizability (in units of 10^{-24} cm^3).

The ion-neutral collision frequency, ν_{in}, used in the calculation of the incoherent scatter spectrum is the momentum transfer collision frequency measured in the laboratory frame:

$$\nu_{in} = \frac{m_n}{m_i + m_n} \bar{\nu}_{in} \quad (2)$$

where m_i and m_n are the ion and neutral particle masses (in atomic mass units), respectively. Combining (1) and (2) and summing over the three principal neutral species in the *E* region, we obtain

$$\nu_{in} = KN \quad (3)$$

for each ion species, where *N* is the total neutral density,

$$K = 2.59 \times 10^{-11}(1/m_i)[1.76^{1/2}\mu(i, \mathrm{N_2})^{1/2}\%(\mathrm{N_2}) + 1.59^{1/2}\mu(i, \mathrm{O_2})^{1/2}\%(\mathrm{O_2}) + 0.79^{1/2}\mu(i, \mathrm{O})^{1/2}\%(\mathrm{O})] \quad (4)$$

and %(*n*) represents the percentage of neutral species *n* in the neutral gas. Equations (3) and (4) indicate that each ion will have a different collision frequency. In addition, the incoherent scatter spectrum is a nonlinear combination of the spectra for each ion. However, the two principal ions in the *E* region, NO^+ and $O_2{}^+$, are close enough in mass that negligible error is introduced in the total ion-neutral collision frequency by assuming one ion with an intermediate mass.

We consider an ion population composed of 75% NO^+ and 25% $O_2{}^+$, thereby obtaining

$$K = \frac{2.59 \times 10^{-11}}{30.5} [5.07\%(\mathrm{N_2}) + 4.98\%(\mathrm{O_2}) + 2.88\%(\mathrm{O})] \quad (5)$$

In the remainder of the paper we continue to use the symbol ν_{in}, but it now represents the total ion-neutral collision frequency.

We can see that the factor *K* depends on the neutral composition (thus on the altitude) and especially on the percentage of atomic oxygen. If we use the "Jacchia 71" neutral model with an exospheric temperature of 1000 K, a 7% difference is obtained between 90 km and 110 km. While this small difference with altitude could vary with the choice of model atmosphere, it would remain small. However, the magnitude of *K* is less certain. It could vary because of atomic oxygen concentration variations as large as a factor of 4 to 5 that have been observed in this region [*Offermann et al.*, 1981]. More fundamentally, (1) is limited because it includes only a pure polarization interaction.

Because of the small variation of *K* with altitude, we will consider it constant, especially when compared with the precision of the collision frequency measurements. We note that the value used in the "EPEC" routines, which compute Joule heating and electric fields from Chatanika data [*de la Beaujardière et al.*, 1980], is 3.75×10^{-10}. This value corresponds to more than 25% atomic oxygen. In the following sections we shall present collision frequencies instead of neutral densities so that no additional error is introduced by the use of the factor *K*.

2.3. *Experimental Conditions*

The data that are presented here were acquired at Chatanika during the joint American-French plasma line experiments in March and November 1978 [*Kofman and Wickwar*, 1980]. We use autocorrelation function measurements obtained with the multipulse correlator in its 60-μs pulse configuration with a 9-km altitude resolution. The time resolution was 15 min, and almost all the data were acquired at night. The radar was pointing along the magnetic field line (in a fixed position), which did not allow electric field measurements.

We have seen that in the auroral zone it is necessary to work during periods without strong electric fields in order to deduce the neutral temperature and the collision frequency. Because these high electric field periods are also characterized by strong Joule heating that enhances the ion temperature T_i at altitudes above 120 km, we have used multipulse measurements immediately above 120 km (where we can indeed determine both T_i and T_e because collisions are no longer important) and single long-pulse measurements in the *F* region to determine Joule heating periods, i.e., periods during which T_i was enhanced above its quiet time value. These periods have been systematically eliminated prior to analysis for neutral temperature and collision frequency.

3. MEAN PROFILES OF COLLISION FREQUENCY AND TEMPERATURE BETWEEN 90 KM AND 110 KM

First we obtained the mean collision frequency and temperature profiles for March and for November 1978. Seventeen

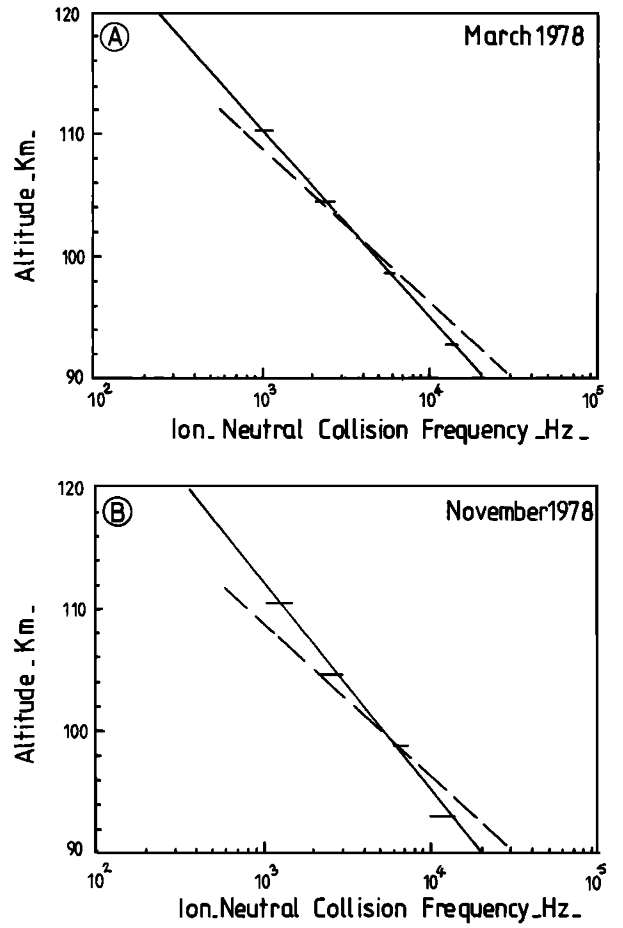

Fig. 1. Mean profiles of collision frequencies deduced from March 1978 and November 1978 measurements. The dotted line is computed from the Jacchia 71 model.

hours of nighttime data were chosen between March 13 and 20 and 8 hours were chosen between November 17 and 25. Values of ν_{in} and T_n were derived from autocorrelation functions, which were integrated for 15 min, using the regression routine ACFIT that is described by *de la Beaujardière et al.* [1980]. Sixty-eight values of ν_{in} and T_n were averaged to obtain the mean profiles for March and 32 values for the mean profiles for November. For the computation of the average, each value of ν_{in} (or T_n) was scaled by the inverse square of the corresponding experimental uncertainty. This uncertainty was computed in the ACFIT routine from the errors for each lag of the autocorrelation function [*Lejeune*, 1980; *Lathuillere*, 1981]. Error bars presented in the figures correspond to the standard deviation of the computed average.

3.1. *Collision Frequencies*

The results obtained for March and November 1978 are presented in Figures 1*a* and 1*b*, respectively; the horizontal axis is collision frequency with a logarithmic scale (bars are error bars for each ν_{in} value) and the vertical axis is altitude.

For each profile we have performed a least squares fit with an exponential function, $\nu_{in}(z) = \nu_{in}(z_0) \exp [(z - z_0)/H]$, in order to compute the scale height H for the collision frequencies, i.e., for the neutral atmosphere. The reference altitude z_0 is 90 km. The results of the regression are drawn as solid lines in Figures 1*a* and 1*b*.

While the collision frequencies at the reference height are almost equal for the two months ($2.12 \times 10^4 \pm 0.11 \times 10^4$ in March and $1.94 \times 10^4 \pm 0.23 \times 10^4$ in November), the scale heights are somewhat different (6.76 ± 0.25 km in March and 7.64 ± 0.59 km in November).

Also drawn in Figures 1*a* and 1*b* (with a dashed line) is the collision frequency profile corresponding to the Jacchia 71 neutral model. Although we have used exospheric temperatures of 800 K and 1200 K, the collision frequency values are the same because the lower boundary conditions of the model are constant. The model scale height is smaller than scale heights for the March and November profiles, but the 98-km and 104-km model values and experimental values agree quite well.

3.2. *Neutral Temperatures*

Neutral temperature profiles for March and November 1978 are displayed in Figures 2*a* and 2*b*, respectively. As previously, horizontal bars represent error bars for each mean temperature. The Jacchia 71 model temperatures corresponding to an exospheric temperature of 1000 K are included for comparison (dashed line). The temperatures observed in March and November are not very different from those of the model.

3.3. *Consistency of the Results*

The mean temperatures and collision frequencies shown above agree well with the Jacchia 71 model. Indeed, in each

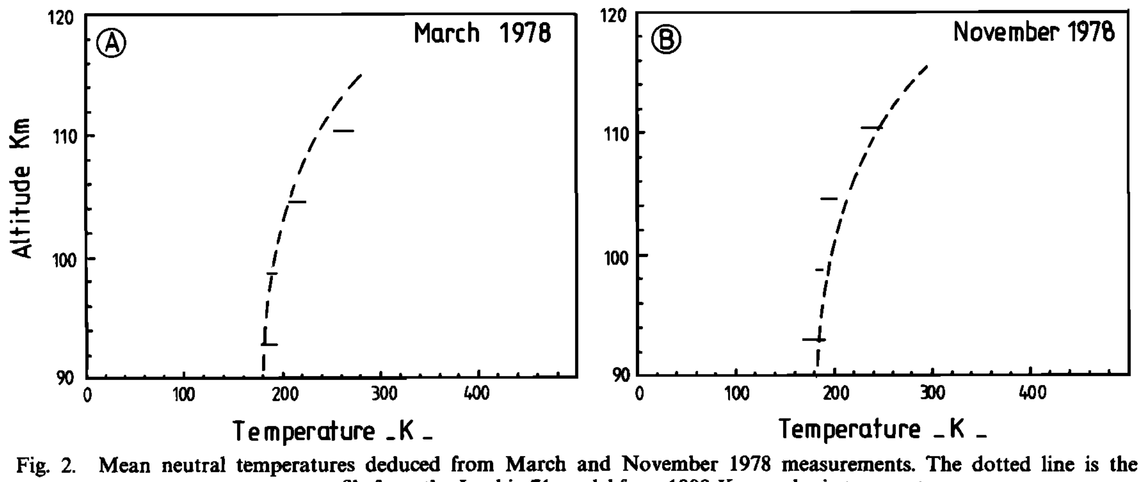

Fig. 2. Mean neutral temperatures deduced from March and November 1978 measurements. The dotted line is the temperature profile from the Jacchia 71 model for a 1000-K exospheric temperature.

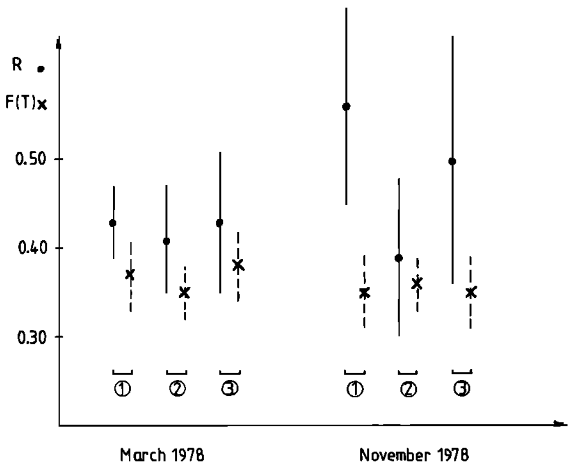

Fig. 3. Comparisons of neutral density ratios obtained from collision frequency measurements (R) and temperature measurements ($F(T)$). Numbers 1 to 3 correspond to the three pairs of measurement altitudes.

case half the points agree with the model. However, the scale heights computed from the collision frequency measurements are greater than the model ones. In order to examine this apparent discrepancy, or, more importantly, to examine the consistency of the temperatures and collision frequencies, we rewrite the equation for hydrostatic equilibrium of the neutral atmosphere in the following form:

$$\frac{N(z_2)}{N(z_1)} = \exp - \left[\frac{Mg}{RT}(z_2 - z_1) + \frac{T_2 - T_1}{T}\right] \quad (6)$$

[*Waldteufel*, 1970*b*], where T, M, and g are the mean values of the neutral temperature, the molecular mass, and the gravitational acceleration between the altitudes z_2 and z_1. $N(z_2)$ and T_2 ($N(z_1)$ and T_1) are the neutral density and temperature at the altitude z_2 (z_1).

For the evaluation of this equation, we take a constant mass M equal to 27.64 amu, i.e., the value of the Jacchia 71 model at the mean altitude of the measurements, 100 km. The error that we introduce is negligible in comparison with the measurement uncertainty. This assumption, which is equivalent to our previous assumption of a constant K parameter, allows us to consider the density ration $N(z_2)/N(z_1)$ equal to the collision frequency ratio $R = \nu_{in}(z_2)/\nu_{in}(z_1)$. The right-hand side of the equation is calculated from the measured temperatures and called $F(T)$. Figure 3 presents the results obtained for three measurement altitude pairs:

$z_1 = 92.8$ km	$z_1 = 98.7$ km	$z_1 = 104.5$ km
$z_2 = 98.7$ km	$z_2 = 104.5$ km	$z_2 = 110.4$ km

For each pair z_1, z_2 the g value is the value of the mean altitude $(z_1 + z_2)/2$. The dots represent the R values, and the crosses represent the corresponding $F(T)$ values. Thus Figure 3 shows consistency between the temperature and collision frequency determinations when error bars are taken into account.

Another way to check the consistency of the results is to determine whether systematic errors can be introduced by the measurement technique. The Chatanika multipulse correlator performs a 9-km altitude integration, which is larger than the scale height of the neutral atmosphere. To check this possible source of error, we simulated the measurements. Theoretical autocorrelation functions (ACF) of the ionospheric medium were computed with a 1.5-km altitude resolution using different neutral temperature profiles and the corresponding ion collision frequency profiles. These values were obtained from the analytical static model of the neutral atmosphere developed by *Alcayde* [1981]. Then the spatial average of these theoretical ACF's was computed in the same way as in the correlator. The theoretical "mean" ACF's at five altitudes close to the real measurement altitudes were analyzed to obtain the "mean" collision frequencies and temperatures.

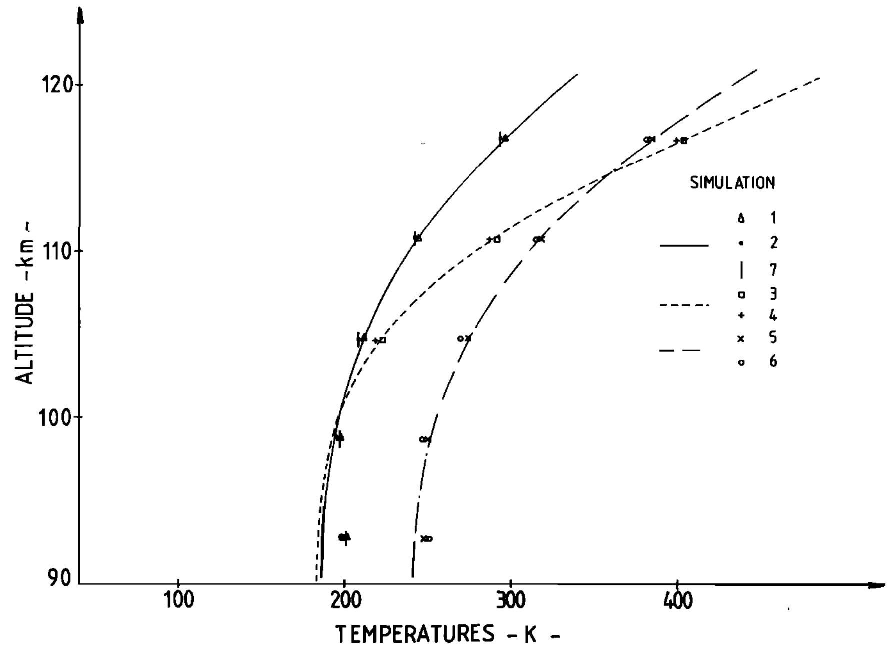

Fig. 4. Results of the altitude integration simulations: the temperature profiles used for the simulation are represented by lines, and the temperatures obtained by symbols.

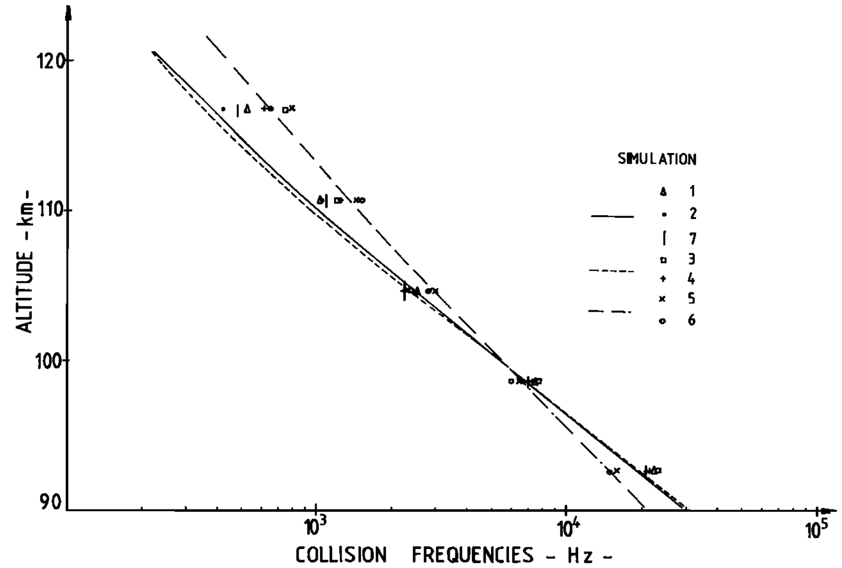

Fig. 5. Same as Figure 4, but for collision frequencies.

Results from these simulations are presented in Figures 4 and 5, which display temperature and collision frequencies, respectively. Simulations 1, 2, and 7 were made with a temperature profile equivalent to the Jacchia 71 neutral model (with an exospheric temperature of 1000 K); simulations 3 and 4, with a model corresponding to the experimental mean profile of March 1978; and simulations 5 and 6, with a model of a very warm atmosphere [*Alcayde*, 1981]. For simulations 1, 3, 5, and 7 the electron density was assumed constant throughout the *E* region. In contrast, simulations 2, 4, and 6 were made with a density profile corresponding to the average of the March 1978 data, i.e., with the *E* layer maximum at 105-km altitude. In addition, in simulation 7 we have included a nonconstant ion velocity profile (variations from 10 to 100 m/s over the 9-km altitude range) in order to evaluate the effects of strong wind shears.

Figure 4 shows that the mean temperatures obtained by the simulations (represented by symbols) are in very good agreement with the model (represented by lines); only at 93 km are they a little overestimated. The collision frequency estimates (represented by symbols in Figure 5) are more scattered, but the error is always less than 15% at the three lowest measurement altitudes. This error is small in comparison with the experimental uncertainties. Above 105 km the worst estimates come from simulations 2 and 3, where the temperature and collision frequency gradients are larger than those in the other cases. These gradients give rise to the larger errors. In contrast to the large influence of the neutral model of the ν_{in} determination, the electron density profile has very little effect. Furthermore, simulation 7 shows that strong wind shears have no noticeable effect on the mean collision frequencies and temperatures.

For these simulations we have not added noise. Therefore the "mean" values obtained represent the bias due to the altitude integration. The receiver noise would add some scatter centered on our simulated values. We have also assumed that the return signal was received through an infinite bandwidth filter. The influence of a finite bandwidth filter would lead to a greater mixing of the contribution from each altitude. Thus our simulations overestimate the errors introduced by the altitude integration.

4. Neutral Temperature and Collision Frequency Variation

For this study we chose four consecutive nights in March 1978: March 16, 17, 18, and 19 during which the experiment was performed from approximately 0800 UT to 1600 UT. After removing Joule heating periods (indicated by solid areas in Figure 6), each night was divided in two parts corresponding to measurements made before 1200 UT (i.e., 0200 hours local time) and after 1200 UT. The exact measurement periods are indicated in Figure 6 (crosshatched areas). Temperature and collision frequency data were then averaged to obtain two data points for each night.

In Figure 6 we used a solid line to depict the 3-hourly magnetic index *Kn*, which represents the magnetic activity over the northern auroral oval (left scale). Corresponding to the right scale, the dotted line depicts the maximum signal-to-noise ratio obtained with the multipulse correlator between the altitudes of 98 km and 110 km. This signal-to-noise ratio is proportional to the electron density and is a local measurement of the auroral particle precipitation at Chatanika.

The four nights that we chose are characterized by different behaviors. During the nights of March 16 and 17, there is an enhancement of the magnetic index and of the local precipitation. On March 18 the magnetic index and local precipitation are constant and quite great during the two measurement periods. In contrast, during the night of March 19, the magnetic index is constant when there is an important enhancement of the local precipitation.

4.1. *Ion-Neutral Collision Frequencies*

In order to characterize the collision frequency profiles, we have chosen the scale height estimated by a least squares fitting procedure identical to the one used for the mean profiles presented in the preceding section. On March 16 and 17, collision frequency values were not obtained at 93 km. Therefore to do the fit, we used the mean collision frequency value previously found at this altitude for this month. For each part of the night we have presented the scale heights in Figure 7. The values are all between 6 km and 8 km.

Scale height variations between the two parts of each night are within the error bars. Thus no variation greater than 15%

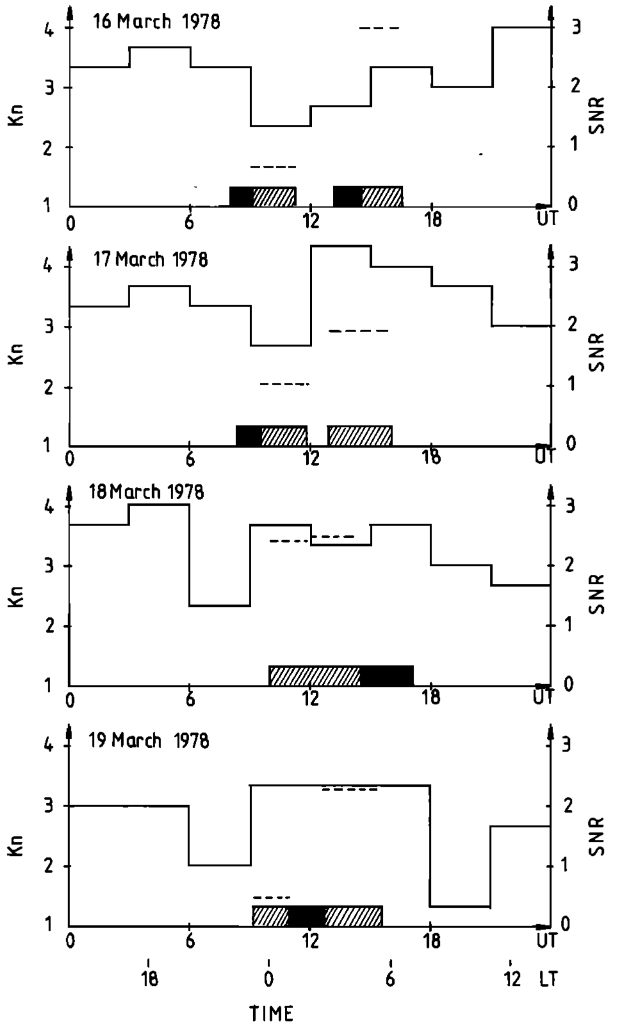

Fig. 6. Periods of measurement used for this study of temperature and collision frequency variation (crosshatched area). Periods of Joule heating, which were not used for this study, are indicated by solid areas. The solid line and the left scale give the *Kn* index; the dashed line and the right scale give the mean signal-to-noise ratio of the measurements.

is found in the scale height for the 93- to 110-km region between late evening and early morning. As a result of the fitting procedure, we also obtain the value of the collision frequency at 90-km altitude. Again, the data points are scattered around the value of the collision frequency obtained for the month of March, and the variations stay within the error bars.

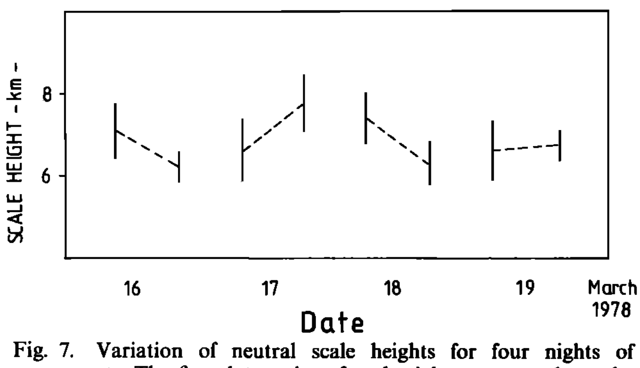

Fig. 7. Variation of neutral scale heights for four nights of measurements. The first data point of each night corresponds to the period prior to 1200 UT; the second, to the period after 1200 UT.

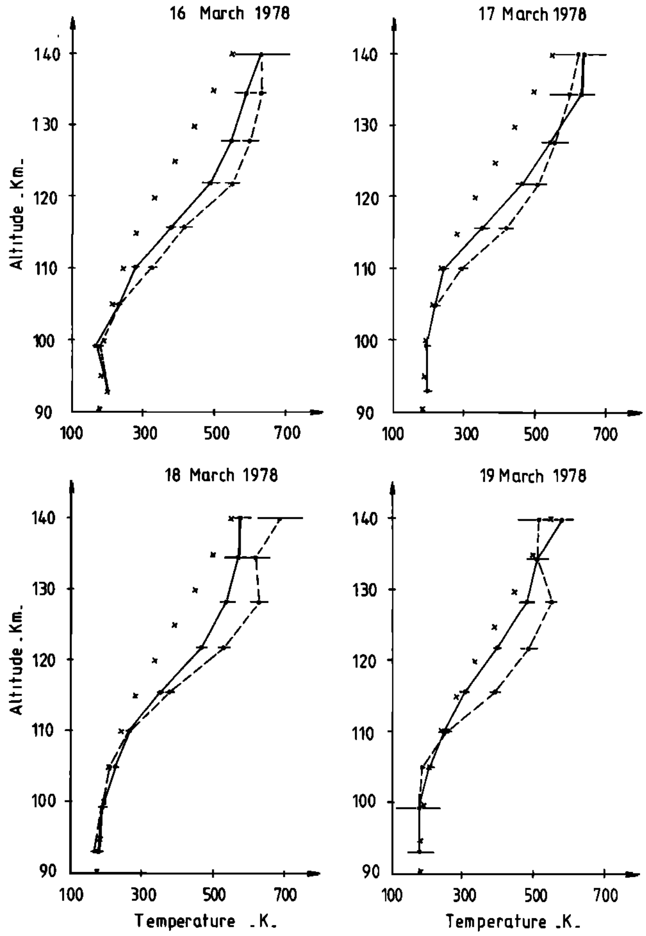

Fig. 8. Variations of neutral temperature profiles for four nights of measurements. The solid line and dashed line correspond to the periods prior to and after 1200 UT, respectively. Crosses are temperature from the Jacchia 71 model for a 1000-K exospheric temperature.

4.2. *Neutral Temperatures*

Ion temperature profiles measured during each night are presented in Figure 8. The solid line represents the profile corresponding to the first part of the night, and the dotted line is the profile corresponding to the second part. Crosses correspond to the Jacchia 71 neutral temperature model calculated with an exospheric temperature of 1000 K. Below 120 km the temperatures displayed correspond to the assumption of thermal equilibrium between ions and electrons. Above this altitude, we assumed a noncollisional medium, but the electron-to-ion ratio was variable. While no ambiguity exists in interpreting the ion temperature as the neutral temperature below 110 km (see section 2), there may be above this altitude because of Joule heating. Therefore, as usual, periods of Joule heating were removed from our data before averaging. Furthermore, we verified that ion temperatures were lower than electron temperatures. Only during the second part of the night of March 18 was T_i 30 K higher than T_e at the altitudes of 122 km and 128 km, which means that there was perhaps a small contribution of Joule heating still present.

Under these conditions, thermal equilibrium between ions and neutrals seems to us to be still justified. Thus we interpret these measured ion temperatures as the neutral temperatures in the lower thermosphere.

Several inferences then can be drawn from Figure 8:

1. There is a good agreement between both sets of experimental temperatures and the Jacchia 71 model below 110 km.

2. At and above 110 km the experimental profiles are more variable and the temperatures greater than those in the model.

3. We have not been able to make any correlation between these variations and the magnetic activity described before.

4. We found a systematic temperature increase between the first and the second part of each night. The maximum of this variation (14% to 20%) is located between the altitudes of 115 km and 125 km.

It is beyond the scope of this paper is make an exhaustive study of this nighttime temperature increase, but we suggest that it can be attributed to the tidal process at equinox. Indeed, while there are no observations of atmospheric tides at high latitude, many studies at middle and low latitudes with three incoherent scatter radars [*Bernard*, 1974; *Salah et al.*, 1975; *Wand*, 1976] support the preponderance of a semidiurnal tide in the *E* region whose main characteristics (vertical wavelength of 40 to 60 km and amplitude of 10 to 20%) correspond to our observations.

5. CONCLUSION

After reviewing how the incoherent scatter technique allows an experimental approach to the study of the lower thermosphere, we have discussed the conditions peculiar to the auroral regions. During periods of large electric fields, which produce Joule heating of the ions and low-altitude electron heating, we are unable to deduce neutral temperatures and densities from the incoherent scatter data.

Our study is the first one of collision frequencies and temperatures in the auroral *E* region based on a large set of data (more than 30 hours) where the altitude integration of the data is almost as small as the neutral scale height.

We showed that the mean collision frequencies are similar to those deduced from the "Jacchia 71" neutral model and that the temperatures are in very good agreement with this model. A consistency check of the temperature and collision frequency data, assuming hydrostatic equilibrium, and a detailed simulation of the data support the results. In addition, possible wind shears as large as 100 m/s in 9 km have no effect on the deduced parameters.

The study of neutral temperatures between 90 km and 140 km during four nights of March 1978 has shown that besides a mean profile that was variable from one night to another, there was a systematic increase during the night, which we suggest is the effect of atmospheric tides.

In the future, additional results on the high-latitude lower thermosphere should be obtainable from the EISCAT and Sondrestrom radars. They will be more sensitive than Chatanika and, by using coded pulses, will have the possibility of better altitude resolution.

Acknowledgments. We gratefully acknowledge many fruitful discussions with G. Lejeune. We would also like to thank the staff members at SRI International and CEPHAG who made these joint experiments and collaboration possible. In particular, we would like to thank J. Kelly, M. McCready, C. Code, and C. D. Feken for their assistance at Chatanika and C. Dawson and C. Leger for their programing work. The French portion of the experiment was supported by the Actions Thématiques Programmées of the Centre National de la Recherche Scientifique for the International Magnetospheric Study. It was supported, as well, by the Centre de Recherche en Physique de l'Environnement Terrestre et Planétaire and by the Centre National d'Etudes des Télécommunications. The American portion was supported by grants ATM7800129 and ATM8121671 from the Aeronomy Program, Division of Atmospheric Sciences, National Science Foundation. In addition, the Chatanika radar was operated by SRI International under contract DNA0001-77-C-0042 from the Defense Nuclear Agency and grant ATM72-01644-A05 from the Division of Atmospheric Science, National Science Foundation.

The Editor thanks K. Schlegel and J. P. St. Maurice for their assistance in evaluating this paper.

REFERENCES

Alcayde, D., An analytic static model of temperature and composition from 20 to 2000 km altitude, *Ann. Geophys.*, *37*, 515–528, 1981.

Alcayde, D., J. Fontanari, G. Kockarts, P. Bauer, and R. Bernard, Temperature, molecular nitrogen concentration and turbulence in the lower thermosphere inferred from incoherent scatter data, *Ann. Geophys.*, *35*, 41–51, 1979.

Banks, P. M., and G. Kockarts, *Aeronomy*, Academic, New York, 1973.

Bernard, R., Tides in the *E* region observed by incoherent scatter radar over St. Santin, *J. Atmos. Terr. Phys.*, *36*, 1105–1120, 1974.

de la Beaujardière, O., V. Wickwar, C. Leger, M. McCready, and M. Baron, The software system for the Chatanika incoherent scatter radar, SRI tech. rep., SRI Int., Menlo Park, Calif., 1980.

Dougherty, J. P., and D. T. Farley, A theory of incoherent scattering of radio waves by a plasma, *J. Geophys. Res.*, *68*, 5473–5486, 1963.

Hedin, A. E., et al., A global thermospheric model based on mass spectrometer and incoherent scatter data, 1, N_2 density and temperature, *J. Geophys. Res.*, *82*, 2139–2147, 1977*a*.

Hedin, A. E., C. A. Reber, G. P. Newton, N. W. Spencer, H. C. Brinton, and H. G. Mayr, A global thermospheric model based on mass spectrometer and incoherent scatter data, 2, Composition, *J. Geophys. Res.*, *82*, 2148–2156, 1977*b*.

Jacchia, L. G., Revised static models of the thermosphere and exosphere with empirical temperature profiles, *Spec. Rep. 322*, Smithson. Astrophys. Observ., Cambridge, Mass., 1971.

Jacchia, L. G., Thermospheric temperature, density and composition: New models, *Spec. Rep. 375*, Smithson. Astrophys. Observ., Cambridge, Mass., 1977.

Kofman, W., and V. B. Wickwar, Plasma line measurements at Chatanika with high-speed correlator and filter bank, *J. Geophys. Res.*, *85*, 2998–3012, 1980.

Lathuillere, C., Experimental study of the uncertainties in incoherent scatter estimation using the ACFIT routine and Chatanika data, *Rep. CEPHAG*, Grenoble, France, 1981.

Lejeune, G., Détermination des incertitudes sur les paramètres measurés par diffusion incohérente, in *Le système EISCAT et l'Etude du Couplage Magnétosphère-Ionosphère-Atmosphère*, edited by D. Alcayde, Centre d'Etude Spatiale des Rayonnements, Toulouse, France, 1980.

Mayr, H. G., and H. Volland, Magnetic storm characteristics of the thermsophere, *J. Geophys. Res.*, *78*, 2251–2264, 1973.

Offermann, D., V. Friedrich, P. Ross, and U. Von Zahn, Neutral gas composition measurements between 80 and 120 km, *Planet. Space Sci.*, *29*, 747–764, 1981.

Salah, J. E., J. V. Evans, and R. H. Wand, Seasonal variations in the thermosphere above Millstone Hill, *Radio Sci.*, *9*, 231–238, 1974.

Salah, J. E., R. H. Wand, and J. V. Evans, Tidal effects in the *E* region from incoherent scatter radar observations, *Radio Sci.*, *10*, 347–355, 1975.

Schlegel, K., and J. P. St. Maurice, Anomalous heating of the polar *E* region by unstable plasma waves, 1, Observations, *J. Geophys. Res.*, *86*, 1447–1452, 1981.

Schlegel, K., H. Kohl, and K. Rinnert, Temperatures and collision frequency in the polar *F* region measured with the incoherent scatter technique, *J. Geophys. Res.*, *85*, 710–714, 1980.

St. Maurice, J. P., K. Schlegel, and P. M. Banks, Anomalous heating of the polar *E* region by unstable plasma waves, 2, Theory, *J. Geophys. Res.*, *86*, 1453–1462, 1981.

Tepley, C. A., and J. D. Mathews, Preliminary measurements of ion-neutral collision frequencies and the mean temperatures in the Arecibo 80- to 100-km region, *J. Geophys. Res.*, *83*, 3299–3302, 1978.

Vidal-Madjar, D., Gravity waves detection in the lower thermosphere with the French incoherent scatter facility, *J. Atmos. Terr. Phys.*, *40*, 685–689, 1978.

Waldteufel, P., A study of seasonal changes in the lower thermosphere and their implications, *Planet. Space Sci*, *18*, 741–748, 1970*a*.

Waldteufel, P., Une étude par diffusion incohérente de la haute atmosphère neutre, thesis, Fac. des Sci. de Paris, Paris, 1970*b*.

Wand, R. H., Semidiurnal tides in the *E* region from incoherent scat-

ter measurements at Arecibo, *Radio Sci.*, *11*, 641–652, 1976.
Wickwar, V. B., C. Lathuillere, W. Kofman, and G. Lejeune, Elevated electron temperatures in the auroral *E* layer measured with the Chatanika radar, *J. Geophys. Res.*, *86*, 4721–4730, 1981.

W. Kofman and C. Lathuillere, Centre d'Etudes des Phénomènes Aléatoires et Géophysiques, BP 46, 38402 Saint-Martin-d'Hères, France.

V. B. Wickwar, SRI International, 333 Ravenswood Avenue, Menlo Park, CA 94025.

(Received April 26, 1983;
revised July 18, 1983;
accepted August 10, 1983.)